

Analysis of image gathers in factorized VTI media

Debashish Sarkar* and Ilya Tsvankin*

ABSTRACT

Because events in image gathers generated after prestack depth migration are sensitive to the velocity field, they are often used in migration velocity analysis for isotropic media. Here, we present an analytic and numerical study of P-wave image gathers in transversely isotropic media with a vertical symmetry axis (VTI) and establish the conditions for flattening such events and positioning them at the true reflector depth. Application of the weak-anisotropy approximation leads to concise expressions for reflections in image gathers from homogeneous and factorized $v(z)$ media in terms of the VTI parameters and the vertical velocity gradient k_z . Flattening events in image gathers for any reflector dip requires accurate values of the zero-dip NMO velocity at the surface [$V_{\text{nmo}}(z=0)$], the gradient k_z , and the anellipticity coefficient η . For a fixed error in V_{nmo} and k_z , the magnitude of residual moveout of events in image gathers decreases with dip, while the moveout caused by an error in η initially increases for moderate dips but then decreases as dips approach 90°. Flat events in image gathers in VTI media, however, do not guarantee the correct depth scale of the model because reflector depth depends on the vertical migration velocity.

INTRODUCTION

The offset-depth gather (often called the image gather) is obtained after prestack depth migration by representing migrated depth (z) as a function of half-offset (h). If the velocity model is correct, a reflection event is migrated to the same depth for all source-receiver pairs and the corresponding image gather is flat [$z(h) = \text{const}$]. Errors in the velocity model cause the migrated depth to vary with offset, which leads to residual moveout on the image gathers. Because of their high sensitivity to the velocity field, reflections in image gathers provide both a simple visual check and a valuable quantitative diagnostic tool for migration velocity analysis. Velocity estimation using image

For factorized $v(x, z)$ media with a linear velocity variation in both the x - and z -directions, the moveout on image gathers is controlled by $V_{\text{nmo}}(x=z=0)$, k_z , η , and a combination of the horizontal velocity gradient k_x and the Thomsen parameter δ (specifically, $k_x\sqrt{1+2\delta}$). If too large a value of any of these four quantities is used in migration, reflections in the image gathers curve downward (i.e., they are undercorrected; the inferred depth increases with offset), while a negative error results in overcorrection. Lateral heterogeneity tends to increase the sensitivity of moveout of events in image gathers to the parameter η , and errors in η may lead to measurable residual moveout of horizontal events in $v(x, z)$ media even for offset-to-depth ratios close to unity.

These results provide a basis for extending to VTI media conventional velocity analysis methods operating with image gathers. Although P-wave traveltimes alone cannot be used to separate anisotropy from lateral heterogeneity (i.e., k_x is coupled to δ), moveout of events in image gathers does constrain the vertical gradient k_z . Hence, it may be possible to build VTI velocity models in depth by supplementing reflection data with minimal a priori information, such as the vertical velocity at the top of the factorized VTI layer.

gathers (as well as any other technique) typically requires a priori information to reduce the nonuniqueness inherent in this inverse problem.

Existing work on the application of image gathers in velocity analysis is largely restricted to isotropic subsurface models (e.g., Al-Yahya, 1987; Stork, 1992; Liu, 1997; Meng, 1999; Zhu et al., 1998; Brandsberg-Dahl, 2001). For example, Liu (1997) develops an analytic approach for inverting the residual moveout on image gathers and computing corrections (updates) to the velocity model. Ubiquitous evidence for the strong influence of seismic anisotropy on reflection moveout (e.g., Thomsen, 1986; Alkhalifah, 1996; Tsvankin, 2001), however, suggests that flattening of events in image gathers using purely

Manuscript received by the Editor July 14, 2002; revised manuscript received May 5, 2003.

*Colorado School of Mines, Department of Geophysics, Golden, Colorado 80401. E-mail: dsarkar@mines.edu; ilya@dix.mines.edu.
© 2003 Society of Exploration Geophysicists. All rights reserved.

isotropic models can often lead to erroneous velocity fields and distortions in migrated sections.

Common problems caused by ignoring anisotropy in seismic imaging include mis-ties in time-to-depth conversion, failure to preserve dipping energy during dip moveout (DMO) correction, and mispositioning of migrated dipping events (e.g., Banik, 1984; Alkhalifah et al., 1996; Tsvankin, 2001). Jaramillo and Larner (1995) study anisotropy-induced errors in prestack depth migration and show that isotropic migration algorithms fail to flatten image gathers for a wide range of transversely isotropic (TI) models. Recent field-data observations by Peng and Steenson (2001) of image gathers with residual moveout that cannot be removed by conventional isotropic methods corroborate Jaramillo and Larner's (1995) conclusions.

Here, we analyze P-wave image gathers for the most common anisotropic model—transverse isotropy with a vertical symmetry axis (VTI media). In contrast to a single scalar velocity responsible for isotropic P-wave propagation, the kinematic signatures of P-waves in VTI media are governed by three parameters: the vertical velocity V_{P0} and Thomsen's (1986) anisotropic coefficients ϵ and δ (Tsvankin and Thomsen, 1994; Tsvankin, 2001). The goal of this work is to study the residual moveout on image gathers caused by errors in these parameters and to establish the conditions needed to flatten and correctly position events in image gathers for homogeneous and factorized $[v(z)]$ and $v(x, z)$ VTI media.

A medium is called factorized if all ratios of the stiffness elements c_{ij} are constant, which implies that anisotropic coefficients and the ratio of the vertical velocities of P- and S-waves must be constant as well. Despite its limitations, the factorized VTI model offers the simplest way to account for both heterogeneity and anisotropy in subsurface formations. For P-waves, velocity heterogeneity in factorized media is described by the spatially varying vertical velocity V_{P0} , while anisotropy is controlled by the constant values of ϵ and δ . Although V_{P0} , ϵ , and δ in the subsurface may vary independently of each other, ϵ and δ are typically estimated with a relatively low spatial resolution. Therefore, a good approximation for realistic VTI velocity fields can often be achieved by dividing the model into factorized VTI blocks, which creates piecewise linear functions of V_{P0} and piecewise constant functions of ϵ and δ .

Because in factorized media the ratio of the vertical P- and S-wave velocities (V_{P0}/V_{S0}) is constant, spatial variations of V_{S0} are directly tied to those of V_{P0} . Since P- and S-wave velocity gradients often differ, the factorized model may seem too simplistic for practical applications. The issue with the S-wave vertical velocity V_{S0} , however, does not arise in P-wave velocity analysis discussed here because P-wave kinematics cannot be used to constrain V_{S0} anyway (Tsvankin and Thomsen, 1994; Alkhalifah, 2000; Tsvankin, 2001).

For 2D wave propagation in the $[x, z]$ plane, the function $z(h)$ that defines the migrated depth of an event in an image gather is obtained by solving the following set of equations:

$$\begin{aligned} \tau_s(x_s, x, z) + \tau_r(x, z, x_r) &= t(y, h), \\ \frac{\partial \tau_s}{\partial y} + \frac{\partial \tau_r}{\partial y} &= \frac{\partial t}{\partial y}, \end{aligned} \quad (1)$$

where y is the common midpoint, τ_s is the traveltime from the source (x_s) to the diffraction point (x, z), τ_r is the traveltime from the receiver (x_r) to the point (x, z), and $t(y, h)$ is the

observed total travelttime that depends on the true positions of the diffractor, the source, and the receiver for midpoint y and half-offset h . Generally, equation (1) does not lend itself to closed-form expressions, even for isotropic media (Liu, 1997). Moreover, analytic treatment of image gathers is much more involved in anisotropic media because of the velocity variation with propagation angle and the increased number of medium parameters.

Hence, most analytic solutions in this paper are based on the weak-anisotropy approximation linearized with respect to the parameters ϵ and δ . The linearized equations, which reveal the influence of the VTI parameters on events in image gathers, are verified by performing numerical tests for a representative set of VTI models.

ALGORITHMS FOR MODELING AND PRESTACK DEPTH MIGRATION

The first step in the numerical analysis of image gathers was to generate 2D synthetic seismograms of P-wave reflections in homogeneous and factorized VTI media using the SU (seismic Unix) code susynlvti (Alkhalifah, 1995a). To build the 2D travelttime tables for prestack depth migration, we used the anisotropic ray-tracing algorithm of Alkhalifah (1995b). The traveltimes τ computed along each ray were then extrapolated to adjacent gridpoints using the paraxial approximation described by Gajewski and Pšenčík (1987):

$$\tau(\mathbf{x}) = \tau(\bar{\mathbf{x}}) + p_k(\bar{\mathbf{x}})(x_k - \bar{x}_k) + \frac{1}{2}N_{ik}(\bar{\mathbf{x}})(x_i - \bar{x}_i)(x_k - \bar{x}_k), \quad (2)$$

where \mathbf{x} corresponds to the point where we seek to find the travelttime, $\bar{\mathbf{x}}$ defines the coordinate of the point on the central ray from which the travelttime is extrapolated, \mathbf{p} is the slowness vector $p_k(\bar{\mathbf{x}}) = (\partial\tau/\partial x_k)|_{\bar{\mathbf{x}}}$, and $N_{ik}(\bar{\mathbf{x}}) = (\partial^2\tau/\partial x_k \partial x_i)|_{\bar{\mathbf{x}}}$. Following Gajewski and Pšenčík (1987), the matrix of the second travelttime derivatives N_{ik} can be written as

$$N_{ik} = \frac{\partial p_i}{\partial x_k} = \frac{\partial p_i}{\partial \gamma_j} \left(\frac{\partial x_k}{\partial \gamma_j} \right)^{-1}, \quad (3)$$

where γ_1 is the takeoff angle at the source (usually denoted by ψ) and $\gamma_2 = \tau$. The slownesses $p_k(\bar{\mathbf{x}})$ and the derivatives $\partial p_i/\partial \tau$ and $\partial x_k/\partial \tau$ can be computed while tracing the central ray.

The derivatives $\partial p_i/\partial \psi$ and $\partial x_k/\partial \psi$, however, are evaluated with respect to takeoff angle along the wavefront [for a constant τ], which requires tracing at least one additional (auxiliary) ray. If $\psi + \Delta\psi$ is the takeoff angle of an auxiliary ray, then the derivatives with respect to ψ can be found by linear interpolation for a fixed travelttime τ :

$$\begin{aligned} \frac{\partial p_i}{\partial \psi} &\approx \frac{p_i(\psi + \Delta\psi) - p_i(\psi)}{\Delta\psi}, \\ \frac{\partial x_i}{\partial \psi} &\approx \frac{x_i(\psi + \Delta\psi) - x_i(\psi)}{\Delta\psi}. \end{aligned} \quad (4)$$

After using equations (4) to compute N_{ik} [equation (3)], we calculated the extrapolated traveltimes $\tau(\mathbf{x})$ from equation (2). The travelttime tables were used in a Kirchhoff prestack depth migration code originally designed for isotropic models (Liu, 1997) to generate image gathers in VTI media.

HOMOGENEOUS VTI MEDIUM

To study the trajectory $z(h)$ of a migrated event in an image gather [equation (1)], we applied the weak-anisotropy approximation (Appendix A). For a horizontal reflector embedded in a homogeneous VTI medium, linearization in the parameters ϵ and δ yields

$$\begin{aligned} z_M^2(h) &= \gamma^2 z_T^2 + h^2 V_{P0,M}^2 \left(\frac{1}{V_{\text{nmo},T}^2} - \frac{1}{V_{\text{nmo},M}^2} \right) \\ &+ \frac{2h^4}{h^2 + z_T^2} \left(\eta_M \frac{V_{\text{nmo},T}^2}{V_{\text{nmo},M}^2} - \eta_T \frac{V_{\text{nmo},M}^2}{V_{\text{nmo},T}^2} \right), \quad (5) \end{aligned}$$

where the subscript T refers to the true model and M to the model used for migration, $z_M(h)$ is the migrated depth for the half-offset h , z_T is the true depth of the zero-offset reflection point, $\gamma \equiv V_{P0,M}/V_{P0,T}$ is the ratio of the migration to true vertical velocity, $V_{\text{nmo}} = V_{P0}\sqrt{1+2\delta}$ is the zero-dip NMO velocity, and $\eta \equiv (\epsilon - \delta)/(1 + 2\delta)$ is the anellipticity parameter of Alkhalifah and Tsvankin (1995), responsible for time processing of P-wave data in VTI media with a laterally homogeneous overburden.

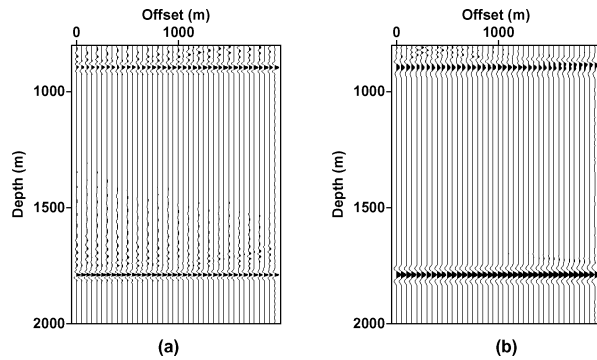


FIG. 1. Image gathers for (a) two horizontal reflectors and (b) two reflectors dipping at 30° embedded in a homogeneous VTI medium. The true model parameters in Figures 1–3 are $V_{P0,T} = 2000$ m/s, $\epsilon_T = 0.1$, and $\delta_T = -0.1$. Prestack depth migration was performed for a model with different values of V_{P0} , δ , and ϵ but with the correct $V_{\text{nmo},M} = V_{\text{nmo},T} = 1789$ m/s and $\eta_M = \eta_T = 0.25$ ($\epsilon_M = 0.25$, $\delta_M = 0$). For this and subsequent figures the maximum offset-to-depth ratio $x_{\max}/z = 2h_{\max}/z$ is equal to two for the shallow reflector (in the true model) and one for the deep reflector.

Equation (5) shows that the moveout of horizontal events on an image gather is fully controlled by the parameters V_{nmo} and η , with V_{nmo} responsible for the near-offset moveout and the influence of η becoming substantial only at large offsets. If the migration and true values of these two parameters are identical ($V_{\text{nmo},M} = V_{\text{nmo},T}$ and $\eta_M = \eta_T$), the migrated depth $z_M(h)$ [equation (5)] is independent of the offset h and the image gather is flat.

Although equation (5) was derived for a horizontal reflector, the correct values of V_{nmo} and η are sufficient for removing residual moveout on image gathers of dipping events as well (see the numerical examples below). This conclusion follows from the general result of Alkhalifah and Tsvankin (1995), who prove that P-wave reflection moveout in VTI media with a laterally homogeneous overburden depends only on the zero-offset traveltimes, V_{nmo} , and η . Positioning an image gather at the true depth, however, requires using the correct vertical velocity ($V_{P0,M} = V_{P0,T}$, which makes $\gamma = 1$).

Figure 1a displays an image gather for two horizontal reflectors embedded in a homogeneous VTI medium at depths of 1000 and 2000 m. The gather was computed for a model with the true parameters $V_{\text{nmo},M} = V_{\text{nmo},T}$ and $\eta_M = \eta_T$ but intentionally includes inaccurate values of the vertical velocity V_{P0} and the coefficients ϵ and δ . Consistent with the conclusions of Alkhalifah and Tsvankin (1995), setting V_{nmo} and η to the correct values ensures that both events in the image gather are flat. The same conditions ($V_{\text{nmo},M} = V_{\text{nmo},T}$ and $\eta_M = \eta_T$) are sufficient to flatten events from dipping reflectors in Figure 1b.

Since the migration was performed with the wrong value of V_{P0} , however, the migrated depths are scaled by the factor $\gamma \approx 0.90$. In agreement with equation (5), the depth of the shallow event is close to 900 m instead of 1000 m, and the deep event is located at 1800 m instead of 2000 m.

For horizontal events, the parameter η contributes only to the far-offset moveout term [equation (5)], which is also true for the P-wave nonhyperbolic reflection moveout equation (Alkhalifah and Tsvankin, 1995; Tsvankin, 2001). Therefore, the influence of η becomes substantial for only relatively large offset-to-depth ratios, i.e., those exceeding unity (Figure 2a). If the reflector is dipping, η contributes to small-offset traveltimes as well because it governs the dip dependence of NMO velocity (Alkhalifah and Tsvankin, 1995; Tsvankin, 2001). Figures 2b and 2c confirm that for dipping events (the dips are 30° and 45°) the residual moveout caused by errors in η is not

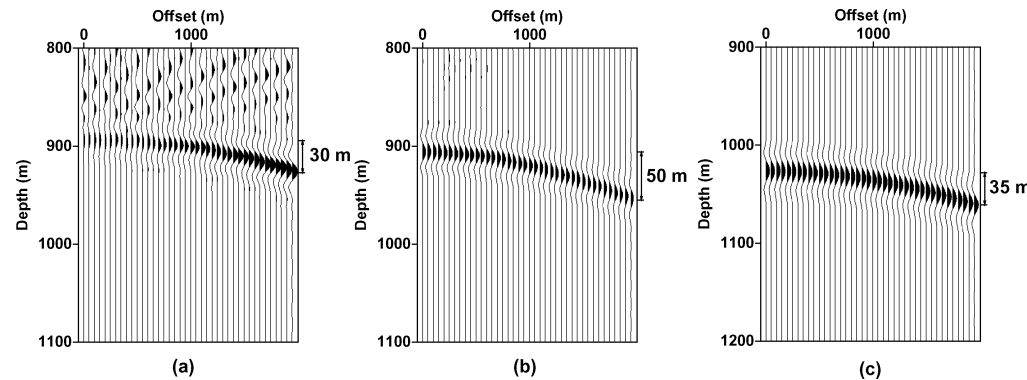


FIG. 2. Image gathers for reflectors dipping at (a) 0°, (b) 30°, and (c) 45° computed for an overstated value of η ($\eta_M = 0.4$, while $\eta_T = 0.25$). Migration was done with the correct V_{nmo} and distorted $\epsilon_M = 0.4$ and $\delta_M = 0$. In the true model the image point has a maximum offset-to-depth ratio of two.

confined to long offsets. The depth error at the largest offset increases from 30 m for the horizontal reflector (Figure 2a) to 50 m for the reflector dipping at 30° (Figure 2b) but then decreases to 35 m for a dip of 45° (Figure 2c); this behavior of residual moveout agrees with the prediction of Jaramillo and Larner (1995). Although the contribution of η to the NMO velocity becomes more significant with dip, the magnitude of reflection moveout decreases for steeper reflectors, which explains this dependence of residual moveout on errors in η .

The NMO velocity in equation (5) not only controls the quadratic term h^2 that dominates the moveout for offsets used in our examples, but it also influences the far-offset moveout term. Hence, an inaccurate value of V_{nmo} leads to significant residual moveout for the whole offset range. For the example in Figure 3, the depth error at the largest offset reaches 80 m for the horizontal reflector, then decreases to 65 m for the 30° reflector and to 45 m for a dip of 45°. This steady decrease in residual moveout with dip for a fixed error in V_{nmo} is caused by the smaller magnitude of reflection moveout and its lower sensitivity to V_{nmo} for larger dips. Liu (1997) noticed this phenomenon for isotropic media, and his analysis remains qualitatively valid in the presence of anisotropy.

FACTORIZED $v(z)$ VTI MEDIUM

Factorized VTI models have spatially varying vertical velocity V_{P0} and constant values of Thomsen's anisotropic coefficients and the V_{P0}/V_{S0} ratio (e.g., Červený, 1989). We consider a subset of factorized VTI models with a linear dependence of the vertical velocity V_{P0} on the coordinates x and z . This section is devoted to vertically heterogeneous models of this type, in which kinematic signatures of P-waves are defined by the velocity V_{P0} at the surface ($z=0$), the vertical-velocity gradient k_z , and the parameters ϵ and δ .

As follows from the results of Appendix B, events in an image gather at the zero-offset time t_0 can be flattened by using the correct values of the NMO velocity (v_{nmo}) and the effective parameter $\hat{\eta}$ given by

$$v_{\text{nmo}}^2(t_0) = \frac{V_{P0}^2(1+2\delta)}{t_0 k_z} [e^{k_z t_0} - 1], \quad (6)$$

$$\hat{\eta}(t_0) = \frac{1}{8} \left\{ \frac{(1+8\eta)(e^{2k_z t_0} - 1)k_z t_0}{2(e^{k_z t_0} - 1)^2} - 1 \right\}, \quad (7)$$

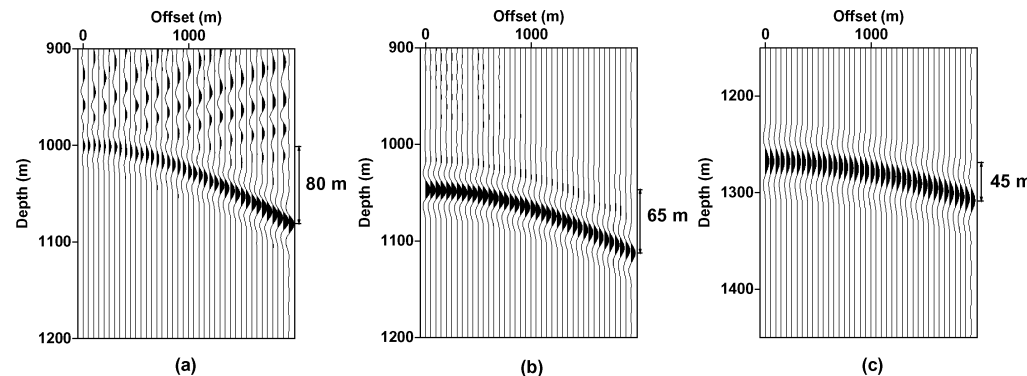


FIG. 3. Image gathers for reflectors dipping at (a) 0°, (b) 30°, and (c) 45° computed for an overstated value of V_{nmo} ($V_{\text{nmo},M}=2000$ m/s, while $V_{\text{nmo},T}=1789$ m/s). Migration was done with the correct η and distorted $\epsilon_M=0.25$ and $\delta_M=0$. In the true model the image point has a maximum offset-to-depth ratio of two.

where t_0 is the zero-offset traveltime. Note that both the NMO velocity and $\hat{\eta}$ are dependent on the vertical gradient k_z . The difference between $\hat{\eta}$ and η and between $v_{\text{nmo}}(t_0)$ and $v_{\text{nmo}}(t_0=0)=V_{P0}\sqrt{1+2\delta}\equiv V_{\text{nmo}}$ increases with k_z .

However, since the vertical velocity in a factorized $v(z)$ medium changes with depth, flattening an event for a certain depth z_r does not ensure that the same velocity model will flatten events for any other depth. To illustrate this point, consider two horizontal reflectors at 1000 and 2000 m depth embedded in a factorized $v(z)$ medium (Figure 4). To migrate data acquired over such a model, we use a homogeneous VTI medium with the parameters chosen such that V_{nmo} and η for the homogeneous model are equal to their effective values for the shallow reflector. As expected, the shallow event in the image gather is flat, but the deeper event exhibits substantial residual moveout because the NMO velocity and η used in migration are too low for a depth of 2000 m.

To ensure that events are flat for the whole depth range of the reflectors, the effective NMO velocity and the parameter $\hat{\eta}$

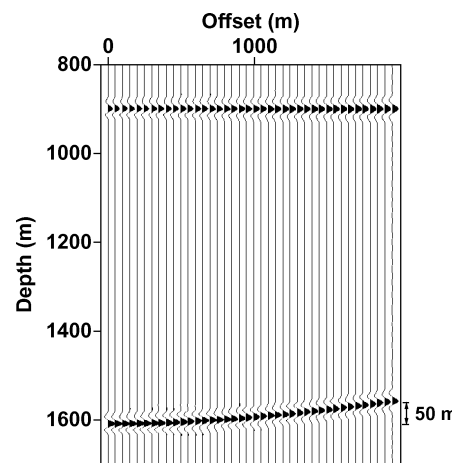


FIG. 4. Image gathers for two horizontal reflectors in a factorized $v(z)$ VTI medium obtained using a homogeneous migration model with the NMO velocity and η equal to the effective values for the shallow reflector. In Figures 4–6 the true parameters are $V_{P0,T}=2000$ m/s, $k_z,T=0.6$ s $^{-1}$, $\epsilon_T=0.1$, and $\delta_T=-0.1$; the parameters used here for the migration are $V_{P0,M}=2054$ m/s, $\epsilon_M=0.26$, and $\delta_M=0$.

for the migration and true models should be equal at all zero-offset times t_0 . Therefore, both the exponential term in equation (6) and the coefficient in front of it should be preserved in the migration model, which means that migration should be done with the correct values of both the NMO velocity at the surface and the vertical gradient: $V_{\text{nmo},M} = V_{P0,M}\sqrt{1+2\delta_M} = V_{P0,T}\sqrt{1+2\delta_T} = V_{\text{nmo},T}$ and $k_{z,M} = k_{z,T}$. Taking into account that $k_{z,M}$ must equal $k_{z,T}$, the condition $\hat{\eta}_M = \hat{\eta}_T$ can be satisfied at all t_0 only if $\eta_M = \eta_T$ [see equation (7)].

We conclude that to flatten all horizontal events in image gathers for a factorized $v(z)$ medium, three conditions need to be satisfied: (1) $V_{\text{nmo},M} = V_{\text{nmo},T}$, (2) $k_{z,M} = k_{z,T}$, and (3) $\eta_M = \eta_T$. Although in principle all three conditions follow from the general result of Alkhalifah and Tsvankin (1995), the results given here for factorized VTI media have not been obtained before. In particular, we show that flattening events for a range of zero-offset times requires using the correct vertical velocity gradient k_z . This implies that velocity analysis on image gathers in VTI media may be used to constrain not just the parameters V_{nmo} and η (as expected) but also k_z .

Figure 5a confirms that if the parameters V_{nmo} , k_z , and η are the same for the migration and true models (although the Thomsen parameters of those models may widely differ), horizontal events in image gathers are flat. Moreover, these three conditions are also sufficient to flatten dipping events (Figure 5b).

The depths in an image gather for a horizontal reflector embedded in a factorized $v(z)$ VTI medium can be described by the following equation (Appendix B):

$$\begin{aligned} z_M^2(h) \approx z_M^2(0) + h^2 \hat{V}_{P0,M}^2 & \left\{ \frac{1}{v_{\text{nmo},T}(z_T)} - \frac{1}{v_{\text{nmo},M}[z_M(0)]} \right\} \\ & + \frac{2h^4}{h^2 + z_T^2} \left\{ \hat{\eta}_M[z_M(0)] \frac{v_{\text{nmo},T}^2(z_T)}{v_{\text{nmo},M}^2[z_M(0)]} \right. \\ & \left. - \hat{\eta}_T(z_T) \frac{v_{\text{nmo},M}^2[z_M(0)]}{v_{\text{nmo},T}^2(z_T)} \right\}. \end{aligned} \quad (8)$$

Here, $z_M(0) = \gamma z_T$, $\gamma \equiv \hat{V}_{P0,M}/\hat{V}_{P0,T}$, and \hat{V}_{P0} is the average vertical velocity above the reflector. Equation (5), obtained for

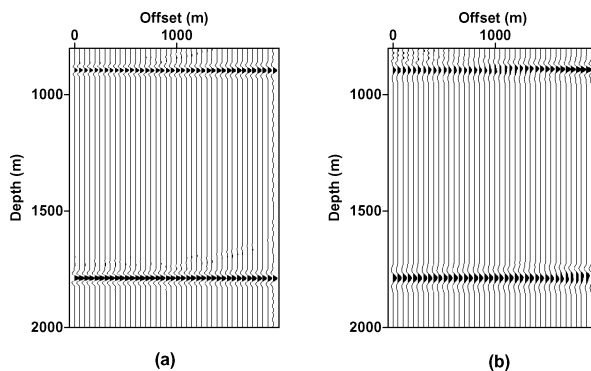


FIG. 5. Image gathers for (a) two horizontal reflectors and (b) two reflectors dipping at 30° embedded in a factorized VTI medium. Prestack depth migration was performed for a model with distorted Thomsen parameters but one that has the correct $V_{\text{nmo},M} = V_{\text{nmo},T} = 1789$ m/s, $k_{z,M} = k_{z,T} = 0.6$ s $^{-1}$, and $\eta_M = \eta_T = 0.25$ ($\epsilon_M = 0.25$, $\delta_M = 0$, $\epsilon_T = 0.1$, $\delta_T = -0.1$).

moderate offsets and under the assumption that the migration model is close to the true model, has the same form as the corresponding expression (5) for homogeneous media. Note that the reflector depth is scaled by the factor γ , which in heterogeneous media depends on the ratio of the average vertical velocities in the migration and true models ($\gamma \approx 0.9$ in Figure 5).

Because of the similarity between equations (5) and (8), the influence of errors in V_{nmo} or η on image gathers in factorized $v(z)$ media resembles that for homogeneous media. Therefore, we focus on the sensitivity of image gathers in the $v(z)$ model to the gradient k_z . Figure 6 illustrates the distortions of image gathers of horizontal events resulting from errors in k_z . Too large a value of k_z leads to an erroneously high NMO velocity and an event in the image gather is undercorrected (Figure 6a), while choosing $k_{z,M} < k_{z,T}$ is equivalent to underestimating the NMO velocity (Figure 6b). Since an erroneous k_z causes the corresponding error in the vertical velocity to increase with depth, the residual moveout in Figure 6 is more substantial for the deep event.

The dip dependence of residual moveout for a fixed error in k_z is similar to that observed in a homogeneous medium for an error in V_{nmo} . If for the model in Figure 6 k_z is overstated by 0.15 s $^{-1}$, the residual moveout decreases from 40 m for the shallow horizontal reflector to 35 m for a dip of 30° and to 30 m for a dip of 45°.

FACTORIZED $v(x, z)$ VTI MEDIUM

Factorized $v(x, z)$ VTI media with linear velocity variation can be described by five independent parameters: the vertical velocity $V_{P0} = V_{P0}(0, 0)$ defined at zero depth $z = 0$ and lateral location $x = 0$, the velocity gradients k_x and k_z responsible for the linear variation of V_{P0} in the x - and z -directions, respectively, and Thomsen parameters ϵ and δ (for P-waves). If we consider the factorized $v(x, z)$ model as being comprised of narrow vertical strips of $v(z)$ factorized media discussed above, it is natural to assume that image gathers in $v(x, z)$ media will be flat if $v_{\text{nmo},M}(x, t_0) = v_{\text{nmo},T}(x, t_0)$ and $\hat{\eta}_M(x, t_0) = \hat{\eta}_T(x, t_0)$ —not only for all vertical times t_0 but also for all coordinates x .

The influence of weak lateral velocity variation on the NMO velocity in horizontally layered anisotropic media is discussed by Grechka and Tsvankin (1999). They show that the NMO ellipse (for wide-azimuth 3D data) must be corrected for lateral velocity variation by including a term dependent on the second

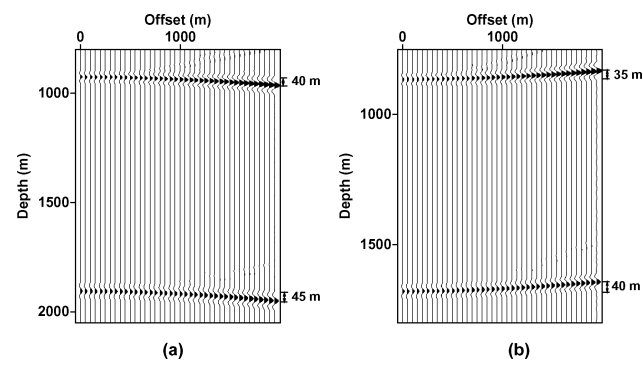


FIG. 6. Image gathers for two horizontal reflectors computed for inaccurate values of the vertical velocity gradient. Migration was done with the correct V_{nmo} and η but with distorted values of k_z . (a) $k_{z,M} - k_{z,T} = 0.15$ s $^{-1}$; (b) $k_{z,M} - k_{z,T} = -0.15$ s $^{-1}$.

derivatives of the vertical velocity with respect to the horizontal coordinates. For the 2D model considered here, the equation of Grechka and Tsvankin (1999) takes the form

$$v_{\text{nmo}}^{-2}(x, z) = v_{\text{nmo,hom}}^{-2}(x, z) + \frac{\tau_0(x, z)}{3} \frac{\partial^2 \tau_0(x, z)}{\partial x^2}, \quad (9)$$

where $v_{\text{nmo,hom}}$ is the NMO velocity in the background laterally homogeneous medium at the coordinate x, z is the reflector depth, and $\tau_0(x, z)$ is the one-way zero-offset reflection travel-time. Since in our model $V_{P0}(x, z)$ and, for weak lateral velocity variation, $\tau_0(x, z)$ are linear functions of x , $v_{\text{nmo}}(x, z)$ from equation (9) is equal to the NMO velocity in the background factorized $v(z)$ medium at the lateral location x . Using equation (B-5), the background NMO velocity can be represented as

$$v_{\text{nmo,hom}}^2(x, z) = \frac{V_{P0}^2(x)(1+2\delta)}{2t_{\text{hom}}(x, z)k_z} [e^{2k_z t_{\text{hom}}(x, z)} - 1], \quad (10)$$

where $V_{P0}(x) = V_{P0} + k_x x$, $t_{\text{hom}}(x, z) = z/\hat{V}_{P0}(x, z)$, and $\hat{V}_{P0}(x, z)$ is the average vertical velocity above the reflector.

As follows from our results for the $v(z)$ model that the v_{nmo} of horizontal events is equal to the true NMO velocity for all vertical times t_0 if the migration is based on the correct values of the vertical velocity gradient k_z and NMO velocity at the surface [$V_{P0}(x)\sqrt{1+2\delta}$]. Hence, $k_{z,M}$ should be equal to $k_{z,T}$, and

$$(V_{P0,M} + k_{x,M}x)\sqrt{1+2\delta_M} = (V_{P0,T} + k_{x,T}x)\sqrt{1+2\delta_T}, \quad (11)$$

which implies that $V_{\text{nmo},M} = V_{P0,M}\sqrt{1+2\delta_M} = V_{P0,T}\sqrt{1+2\delta_T} = V_{\text{nmo},T}$ and $k_{x,M}\sqrt{1+2\delta_M} = k_{x,T}\sqrt{1+2\delta_T}$. Also, because $k_{z,M} = k_{z,T}$, setting $\hat{\eta}_M(x, t_0) = \hat{\eta}_T(x, t_0)$ [equation (7)] for all zero-offset times and lateral positions implies that $\eta_M = \eta_T$.

We conclude that flattening all image gathers of horizontal events in a factorized $v(x, z)$ medium requires satisfying four conditions:

- 1) $V_{\text{nmo},M} = V_{\text{nmo},T}$,
- 2) $k_{z,M} = k_{z,T}$,
- 3) $\eta_M = \eta_T$, and
- 4) $k_{x,M}\sqrt{1+2\delta_M} = k_{x,T}\sqrt{1+2\delta_T}$.

The first three conditions coincide with those obtained for $v(z)$ media; condition four is an additional constraint on the horizontal velocity gradient combined with the parameter δ . Even in the presence of lateral heterogeneity, moveout on image gathers constrains the vertical gradient k_z . While estimation of k_z is feasible, the individual values of the horizontal gradient k_x and the parameters V_{P0} , ϵ , and δ remain unconstrained and cannot be found using P-wave reflection moveout alone.

As illustrated in Figure 7a, the conditions listed above indeed ensure that the horizontal events are flat, even if the migration is done with erroneous model parameters. Because an incorrect vertical velocity was used, however, the depths are stretched by the factor equal to the ratio of the migration [$\hat{V}_{P0,M}(t_0)$] and true [$\hat{V}_{P0,T}(t_0)$] average vertical velocities evaluated at the lateral coordinate x of the zero-offset reflection point. Although equation (10) was derived for horizontal reflectors, the same four conditions prove to be sufficient for flattening dipping events in image gathers (Figure 7b).

As was the case in $v(z)$ media, it is impossible to constrain the vertical velocity gradient using a single event because of the trade-off between k_z and the NMO velocity at the surface. In general, removing the residual moveout of one event in an image gather does not guarantee that events at other depths or lateral coordinates will be flat, unless independent information about the vertical and horizontal gradients is available.

Inaccurate values of V_{nmo} , k_z , or $k_x\sqrt{1+2\delta}$ cause an error in v_{nmo} and thus introduce residual moveout on image gathers for the whole offset range. Figures 8–10 illustrate the influence of errors in V_{nmo} and $k_x\sqrt{1+2\delta}$, while errors in k_z are analyzed above for $v(z)$ media (Figure 6). The image gathers are particularly sensitive to the horizontal velocity gradient k_x , with an error in $k_x\sqrt{1+2\delta}$ of just 0.02 s⁻¹ (which translates into an error of 100 m/s in the vertical velocity in this example) creating a substantial residual moveout (Figures 9 and 10). As in homogeneous media, the residual moveout for a fixed error in V_{nmo} , k_z , or $k_x\sqrt{1+2\delta}$ decreases with reflector dip (e.g., see Figures 9a and 10).

It is noteworthy that the magnitude of residual moveout caused by a fixed error in V_{nmo} is smaller in factorized media than in homogeneous media for the same $V_{P0,M}$, $V_{P0,T}$, ϵ_M ,

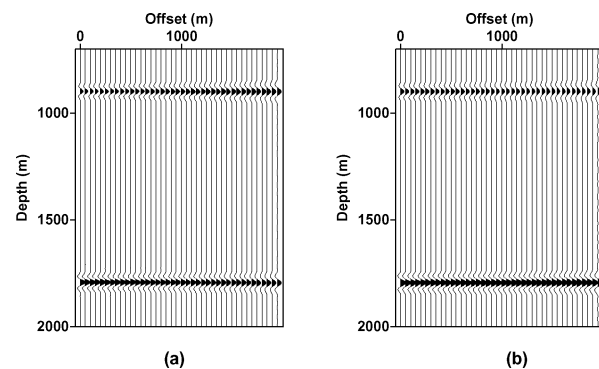


FIG. 7. Image gathers for (a) two horizontal reflectors and (b) two reflectors dipping at 30° embedded in a factorized $v(x, z)$ VTI medium. In Figures 7–12 the true model parameters are $V_{P0,T} = 2000$ m/s, $k_{z,T} = 0.6$ s⁻¹, $k_{x,T} = 0.2$ s⁻¹, $\epsilon_T = 0.1$, and $\delta_T = -0.1$, and the gathers are centered at lateral coordinate $x = 6000$ m. Prestack depth migration was performed for a model with distorted parameters, but one that has the correct $V_{\text{nmo},M} = V_{\text{nmo},T} = 1789$ m/s, $k_{z,M} = k_{z,T} = 0.6$ s⁻¹, $k_{x,M}\sqrt{1+2\delta_M} = k_{x,T}\sqrt{1+2\delta_T} = 0.18$ s⁻¹, and $\eta_M = \eta_T = 0.25$ ($\epsilon_M = 0.25$, $\delta_M = 0$).

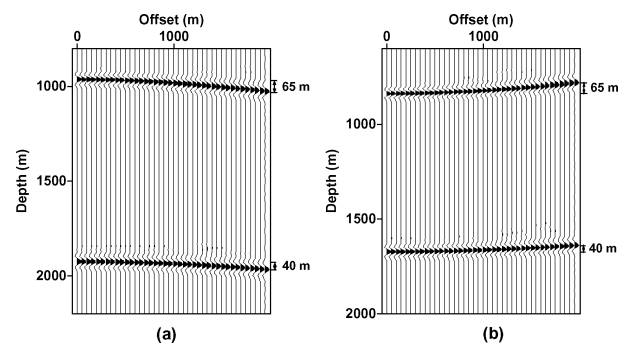


FIG. 8. Image gathers for two horizontal reflectors computed for inaccurate values of V_{nmo} but correct k_z , η , and $k_x\sqrt{1+2\delta_M}$. (a) $V_{\text{nmo},M} - V_{\text{nmo},T} \approx 200$ m/s ($V_{P0,M} = 2000$ m/s, $\delta_M = 0$); (b) $V_{\text{nmo},M} - V_{\text{nmo},T} \approx -200$ m/s ($V_{P0,M} = 1600$ m/s, $\delta_M = 0$).

ϵ_T , δ_M , and δ_T . For example, if the value of V_{nmo} is overstated by 200 m, the residual moveout for the shallow horizontal reflector in a factorized $v(x, z)$ VTI medium reaches 65 m (Figure 8b). If the same reflector is embedded in the reference homogeneous VTI medium, the residual moveout increases to 80 m. Therefore, velocity gradients tend to mitigate the distortions in image gathers caused by errors in V_{nmo} . Likewise, the residual moveout for a fixed error in k_z is smaller in a $v(x, z)$ medium than in the corresponding laterally homogeneous $v(z)$ model. In contrast, the residual moveout associated with errors in η is larger for factorized $v(x, z)$ media than for the reference homogeneous medium (compare Figures 2a and 11a).

The dip dependence of the residual moveout in factorized media for a fixed error in η has the same character as in homogeneous media. For a 0.15 error in η , the residual increases from 40 m for a horizontal reflector (Figure 11a) to 60 m for a reflector dipping at 30° (Figure 12a) and then decreases to 50 m for a 45° dip (Figure 12b).

DISCUSSION AND CONCLUSIONS

In conventional seismic processing for isotropic media, image gathers are a convenient tool for refining velocity models as well as for a quick qualitative assessment of the accuracy of velocity analysis. If the medium is anisotropic, reflection moveout is governed by several anisotropic parameters and the interpretation of image gathers becomes much more complicated. Here, we have presented an analytic and numerical

study of P-wave image gathers in homogeneous and factorized $[v(z)]$ and $v(x, z)$ VTI media.

Using the weak-anisotropy approximation, we have obtained a simple representation of image gathers of horizontal events for homogeneous VTI media in terms of the vertical velocity V_{P0} , the NMO velocity V_{nmo} , and the Alkhalifah-Tsvankin parameter η . Although this equation describes imaged depths, its structure is similar to that of the nonhyperbolic equation for P-wave reflection traveltimes (Alkhalifah and Tsvankin, 1995). The moveout on image gathers depends on the parameters V_{nmo} and η , with the NMO velocity responsible for the small-offset term and η governing the term quartic in offset. Therefore, although in principle the correct values of both V_{nmo} and η are needed to flatten an event, the influence of η becomes substantial only for offset-to-depth ratios exceeding unity.

In agreement with the general result of Alkhalifah and Tsvankin (1995), the same conditions (correct values of V_{nmo} and η) are needed to flatten dipping events in image gathers; but, in the presence of dip, η makes a substantial contribution to the near-offset moveout as well. The magnitude of residual moveout for a fixed error in V_{nmo} decreases with dip, while the residuals caused by an error in η reach their maximum value for intermediate dips (25°–35° in our examples). Even if prestack migration is performed with the correct parameters V_{nmo} and η , and the events are flat and well focused, the imaged depth is scaled by a factor equal to the ratio of the migration and true vertical velocities.

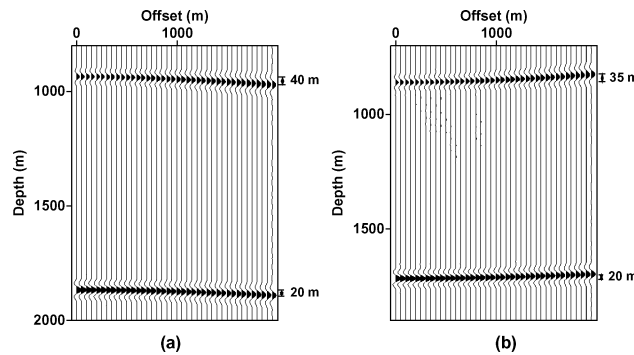


FIG. 9. Image gathers for two horizontal reflectors computed for inaccurate values of $k_x\sqrt{1+2\delta}$ but correct V_{nmo} , k_z , and η_M ($\delta_M=0$). (a) $k_{x,M}\sqrt{1+2\delta_M} - k_{x,T}\sqrt{1+2\delta_T} = 0.02 \text{ s}^{-1}$; (b) $k_{x,M}\sqrt{1+2\delta_M} - k_{x,T}\sqrt{1+2\delta_T} = -0.02 \text{ s}^{-1}$.

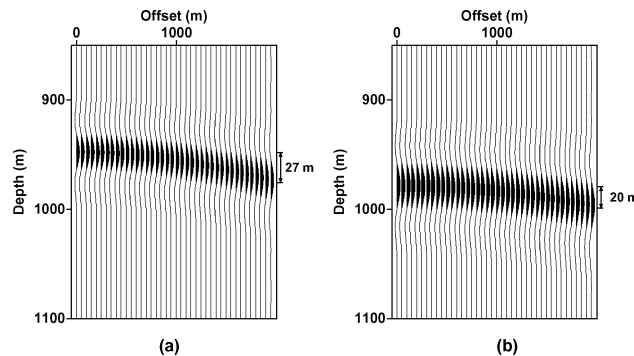


FIG. 10. Image gathers for reflectors dipping at (a) 30° and (b) 45° computed for a value of $k_x\sqrt{1+2\delta}$ overstated by 0.02 but correct V_{nmo} , k_z , and η ($\delta_M=0$).

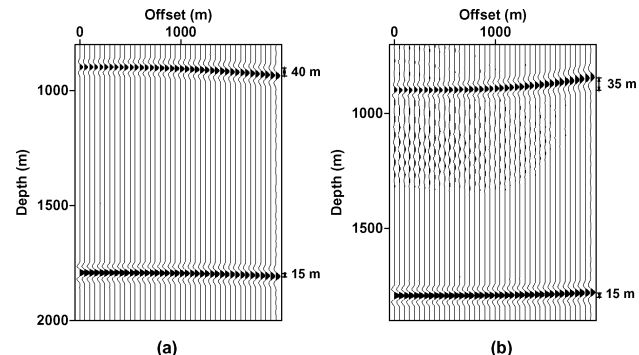


FIG. 11. Image gathers for two horizontal reflectors computed for inaccurate values of η but correct V_{nmo} , k_z , and $k_x\sqrt{1+2\delta}$ ($\delta_M=0$). (a) $\eta_M - \eta_T = 0.15$; (b) $\eta_M - \eta_T = -0.15$.

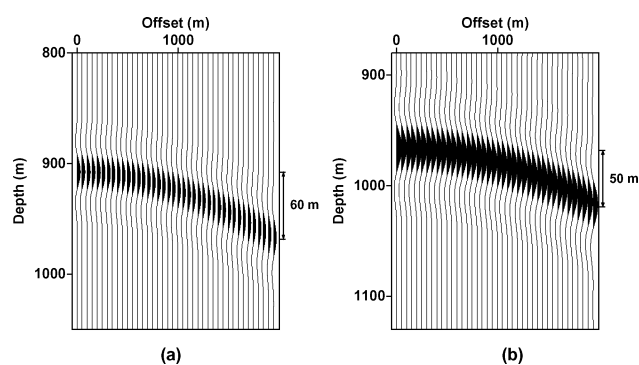


FIG. 12. Image gathers for reflectors dipping at (a) 30° and (b) 45° computed for a value of η overstated by 0.15 but correct V_{nmo} , k_z , and $k_x\sqrt{1+2\delta}$ ($\delta_M=0$).

For factorized $v(z)$ models with a constant vertical velocity gradient k_z , the equation for moveout in image gathers of horizontal events has the same form as that in homogeneous media, but the effective vertical and NMO velocities are now influenced by the vertical velocity gradient. Flattening events with any dip in $v(z)$ media requires the correct values of the NMO velocity at the surface, the coefficient η , and the gradient k_z . The influence of errors in k_z on the residual moveout decreases with dip (as is the case for errors in V_{nmo}) but increases with reflector depth.

Extension of the above results to laterally heterogeneous $v(x, z)$ models is based on the NMO equation of Grechka and Tsvankin (1999), which includes a correction term dependent on the lateral variation of the vertical velocity (or vertical traveltime). For a weak linear velocity dependence on x , the correction term vanishes and the NMO velocity is equal to the corresponding value in the laterally homogeneous background. To equalize the background NMO velocities for all x , migration should be done with the correct value of the parameter combination $k_x \sqrt{1+2\delta}$ (k_x is the horizontal velocity gradient).

Therefore, moveout on image gathers in $v(x, z)$ media is controlled by four parameter combinations: $V_{\text{nmo}}(x=z=0) = V_{P0} \sqrt{1+2\delta}$, η , k_z , and $k_x \sqrt{1+2\delta}$. A positive error in any of these quantities causes undercorrection (i.e., the imaged depth increases with offset) and a negative error causes overcorrection. For a fixed error in $V_{\text{nmo}}(x=z=0)$, the residual moveout in $v(x, z)$ media is smaller than that in the reference homogeneous model, which indicates that lateral heterogeneity is likely to hamper the estimation of this parameter from image gathers. In contrast, the influence of η on residual moveout becomes more substantial in the presence of lateral heterogeneity, and errors in η lead to measurable residual moveout of horizontal events even for offset-to-depth ratios close to unity.

Estimation of these four key parameter combinations requires using several events in image gathers at different depths and lateral positions. Even if all four combinations have been resolved, separation of lateral velocity variation from the anisotropic coefficients (i.e., separation of k_x from δ) cannot be accomplished without additional information.

In contrast, the vertical velocity gradient k_z is constrained by P-wave image gathers not only in the $v(z)$ model but also in laterally heterogeneous media. As a result, although the inversion of P-wave data for the vertical velocity and Thomsen coefficients will suffer from inherent ambiguities, minimal a priori assumptions may be sufficient to remove the trade-offs among the VTI parameters. For example, if the vertical velocity V_{P0} is known at any single surface location (which is quite possible), then the inverted gradient k_z can be used to reconstruct the function $V_{P0}(z)$ and find the depth scale of the model. Also, in this situation, the anisotropic parameter δ can be estimated from the NMO velocity at the surface ($V_{P0} \sqrt{1+2\delta}$) and, in turn, used to determine the horizontal gradient k_x and the parameter ϵ . The feasibility of this parameter-estimation

methodology for different sets of input data and realistic levels of noise will be examined in future publications.

ACKNOWLEDGMENTS

We are grateful to members of the A(nisotropy)-Team of the Center for Wave Phenomena (CWP), Colorado School of Mines, for helpful discussions and to Ken Larner (CSM), Andreas Rüger (Landmark), and the referees of *Geophysics* for their careful reviews of the manuscript. The support for this work was provided by the Consortium Project on Seismic Inverse Methods for Complex Structures at CWP and by the Chemical Sciences, Geosciences and Biosciences Division, Office of Basic Energy Sciences, U.S. Department of Energy.

REFERENCES

- Alkhalifah, T., 1995a, Efficient synthetic-seismogram generation in transversely isotropic, inhomogeneous media: *Geophysics*, **60**, 1139–1150.
- Alkhalifah, T., 1995b, Gaussian beam depth migration for anisotropic media: *Geophysics*, **60**, 1474–1484.
- Alkhalifah, T., 1996, Seismic processing in transversely isotropic media: Ph.D. thesis, Colorado School of Mines.
- Alkhalifah, T., 1997, Velocity analysis using nonhyperbolic moveout in transversely isotropic media: *Geophysics*, **62**, 1839–1853.
- Alkhalifah, T., 2000, An acoustic wave equation for anisotropic media: *Geophysics*, **65**, 1239–1251.
- Alkhalifah, T., and Tsvankin, I., 1995, Velocity analysis for transversely isotropic media: *Geophysics*, **60**, 1550–1566.
- Alkhalifah, T., Tsvankin, I., Larner, K., and Toldi, J., 1996, Velocity analysis and imaging in transversely isotropic media: Methodology and a case study: *The Leading Edge*, **15**, No. 5, 371–378.
- Al-Yahya, K., 1987, Prestack migration velocity analysis: Determination of interval velocities: Stanfold Exploration Project **SEP-51**, 49–61.
- Banik, N. C., 1984, Velocity anisotropy of shales and depth estimation in the North Sea basin: *Geophysics*, **49**, 1411–1419.
- Brandsberg-Dahl, S., 2001, Imaging-inversion and migration velocity analysis in the scattering-angle/azimuth domain: Ph.D. thesis, Colorado School of Mines.
- Červený, V., 1989, Ray tracing in factorized anisotropic inhomogeneous media: *Geophys. J. Internat.*, **99**, 91–100.
- Gajewski, D., and Pšenčík, I., 1987, Computation of high-frequency seismic wavefields in 3-D laterally inhomogeneous anisotropic media: *Geophys. J. Roy. Astr. Soc.*, **91**, 383–411.
- Grechka, V., and Tsvankin, I., 1999, 3-D moveout inversion in azimuthally anisotropic media with lateral velocity variation: Theory and a case study: *Geophysics*, **64**, 1202–1218.
- Jaramillo, H., and Larner, K., 1995, Prestack migration error in transversely isotropic media: CWP Research Report 185.
- Liu, Z., 1997, An analytical approach to migration velocity analysis: *Geophysics*, **62**, 1238–1249.
- Meng, Z., 1999, Tetrahedral based earth models, ray tracing in tetrahedral models and analytical migration velocity analysis: Ph.D. thesis, Colorado School of Mines.
- Peng, C., and Steenson, K. E., 2001, 3-D prestack depth migration in anisotropic media: A case study at the Lodepole reef play in North Dakota: *The Leading Edge*, **20**, 524–527.
- Stork, C., 1991, Reflection tomography in the postmigrated domain: *Geophysics*, **57**, 680–692.
- Thomsen, L., 1986, Weak elastic anisotropy: *Geophysics*, **51**, 1954–1966.
- Tsvankin, I., 2001, Seismic signatures and analysis of reflection data in anisotropic media: Elsevier Science Publ. Co., Inc.
- Tsvankin, I., and Thomsen, L., 1994, Nonhyperbolic reflection moveout in anisotropic media: *Geophysics*, **59**, 1290–1304.
- Zhu, J., Lines, L., and Gray, S., 1998, Smiles and frowns in migration velocity analysis: *Geophysics*, **63**, 1200–1209.

APPENDIX A

IMAGE GATHER FOR A HORIZONTAL REFLECTOR IN A HOMOGENEOUS VTI MEDIUM

Consider a horizontal reflector located at a depth z_T in a VTI medium with vertical velocity $V_{P0,T}$ and Thomsen parameters ϵ_T and δ_T (Figure A-1). Suppose P-wave data acquired over such a model are migrated with the parameters $V_{P0,M}$, ϵ_M , and δ_M . Clearly, for a horizontal reflector the image point does not move laterally. Therefore, the reflection traveltimes in the true (t_T) and migration (t_M) models for the half-offset h can be written as

$$t_T = \frac{2\sqrt{h^2 + z_T^2}}{V_{g,T}(\phi)} \quad (\text{A-1})$$

and

$$t_M = \frac{2\sqrt{h^2 + z_M^2}}{V_{g,M}(\phi')}, \quad (\text{A-2})$$

where $V_{g,T}$ is the group velocity at the group angle ϕ in the true model and $V_{g,M}$ is the group velocity at the group angle ϕ' in the model used for migration.

Under the assumption of weak anisotropy, quadratic and higher order terms in the anisotropic coefficients can be neglected, and the group velocity can be replaced with the corresponding phase velocity (Thomsen, 1986; Tsvankin, 2001):

$$V_{g,T}(\phi) = V_{P0,T} [1 + \delta_T \sin^2 \phi + (\epsilon_T - \delta_T) \sin^4 \phi]. \quad (\text{A-3})$$

Likewise, for the migration model

$$V_{g,M}(\phi') = V_{P0,M} [1 + \delta_M \sin^2 \phi' + (\epsilon_M - \delta_M) \sin^4 \phi']. \quad (\text{A-4})$$

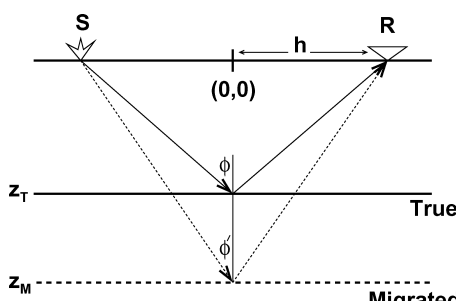


FIG. A-1. True and migrated positions of a horizontal reflector.

Substituting equations (A-3) and (A-4) into equations (A-1) and (A-2), equating the true and migration traveltimes ($t_T = t_M$), and linearizing the resulting expression in the anisotropic coefficients yields

$$\begin{aligned} & \gamma^2(h^2 + z_T^2)[1 - 2\delta_T \sin^2 \phi - 2(\epsilon_T - \delta_T) \sin^4 \phi] \\ &= (h^2 + z_M^2)[1 - 2\delta_M \sin^2 \phi' - 2(\epsilon_M - \delta_M) \sin^4 \phi'], \end{aligned} \quad (\text{A-5})$$

where $\gamma \equiv V_{P0,M}/V_{P0,T}$.

Expressing

$$\sin^2 \phi = \frac{h^2}{h^2 + z_T^2} \quad \text{and} \quad \sin^2 \phi' = \frac{h^2}{h^2 + z_M^2} \quad (\text{A-6})$$

in equation (A-5) and solving for z_M , we obtain

$$\begin{aligned} z_M^2 &\approx \gamma^2 z_T^2 + h^2(2\delta_M - 1 + \gamma^2 - 2\delta_T \gamma^2) \\ &\quad - \frac{2h^4 \gamma^2 (\epsilon_T - \delta_T)}{h^2 + z_T^2} + \frac{2h^4 (\epsilon_M - \delta_M)}{\gamma^2 (h^2 + z_T^2)}. \end{aligned} \quad (\text{A-7})$$

The coefficient of h^2 can be represented as

$$(2\delta_M - 1 + \gamma^2 - 2\delta_T \gamma^2) \approx V_{P0,M}^2 \left(\frac{1}{V_{\text{nmo},T}^2} - \frac{1}{V_{\text{nmo},M}^2} \right), \quad (\text{A-8})$$

where $V_{\text{nmo}} = V_{P0} \sqrt{1+2\delta} \approx V_{P0}(1+\delta)$. Similarly, the coefficient of $[2h^4/(h^2 + z_T^2)]$ takes the form

$$\gamma^2(\epsilon_T - \delta_T) - \frac{(\epsilon_M - \delta_M)}{\gamma^2} \approx \left(\eta_T \frac{V_{\text{nmo},M}^2}{V_{\text{nmo},T}^2} - \eta_M \frac{V_{\text{nmo},T}^2}{V_{\text{nmo},M}^2} \right), \quad (\text{A-9})$$

where $\eta \equiv (\epsilon - \delta)/(1+2\delta) \approx \epsilon - \delta$. Therefore, equation (A-7) can be rewritten in terms of V_{nmo} and η as

$$\begin{aligned} z_M^2 &\approx \gamma^2 z_T^2 + h^2 V_{P0,M}^2 \left(\frac{1}{V_{\text{nmo},T}^2} - \frac{1}{V_{\text{nmo},M}^2} \right) \\ &\quad + \frac{2h^4}{h^2 + z_T^2} \left(\eta_M \frac{V_{\text{nmo},T}^2}{V_{\text{nmo},M}^2} - \eta_T \frac{V_{\text{nmo},M}^2}{V_{\text{nmo},T}^2} \right). \end{aligned} \quad (\text{A-10})$$

APPENDIX B
IMAGE GATHER IN A FACTORIZED $v(z)$ MEDIUM

Here, we extend the results of Appendix A to factorized $v(z)$ VTI media defined by the vertical velocity $V_{P0,T}$ at zero depth, the vertical velocity gradient $k_{z,T}$, and Thomsen parameters ϵ_r and δ_r . The one-way zero-offset time τ for a horizontal reflector can be found as the following function of depth z :

$$\tau = \int_0^z \frac{d\xi}{V(\xi)}$$

$$\begin{aligned} &= \int_0^z \frac{d\xi}{V_{P0,T} + k_{z,T} \xi} \\ &= \frac{1}{k_{z,T}} \ln \left[\frac{V_{P0,T} + k_{z,T} z}{V_{P0,T}} \right]. \end{aligned} \quad (\text{B-1})$$

Expressing z as a function of τ yields

$$z = \frac{V_{P0,T}}{k_{z,T}} (e^{k_{z,T} \tau} - 1). \quad (\text{B-2})$$

Substituting z into the equation $V_{P0,T}(z) = V_{P0,T} + k_{z,T}z$ allows us to represent the vertical velocity as a function of the zero-offset time:

$$V_{P0}(\tau) = V_{P0,T}e^{k_{z,T}\tau}. \quad (\text{B-3})$$

Then the interval NMO velocity is given by

$$V_{\text{nmo}}(\tau) = V_{P0,T}\sqrt{1 + 2\delta_T}e^{k_{z,T}\tau}. \quad (\text{B-4})$$

Applying the Dix formula and substituting equation (B-4), we obtain the effective NMO velocity for a reflector at a depth z_T :

$$\begin{aligned} v_{\text{nmo},T}^2(\tau_0) &= \frac{1}{\tau_0} \int_0^{\tau_0} V_{\text{nmo}}^2(\tau) d\tau, \\ &= \frac{V_{P0,T}^2(1 + 2\delta_T)}{2\tau_0 k_{z,T}} (e^{2k_{z,T}\tau_0} - 1) \end{aligned}$$

or

$$v_{\text{nmo},T}^2(t_0) = \frac{V_{P0,T}^2(1 + 2\delta_T)}{t_0 k_{z,T}} (e^{k_{z,T}t_0} - 1) \quad (\text{B-5})$$

where $t_0 = 2\tau_0$ is the two-way zero-offset time.

As shown in Alkhalifah (1997) and Appendix 4B of Tsvankin (2001), the zero-offset time t_0 , the NMO velocity v_{nmo} , and the parameter $\hat{\eta}$, which is defined as

$$\begin{aligned} \hat{\eta}_T &= \frac{1}{8} \left\{ \frac{(1 + 8\eta_T)}{v_{\text{nmo},T}^4(\tau_0)\tau_0} \left[\int_0^{\tau_0} V_{\text{nmo}}^4(\tau) d\tau \right] - 1 \right\} \\ &= \frac{1}{8} \left\{ \frac{(1 + 8\eta_T)(e^{2k_{z,T}t_0} - 1)k_{z,T}t_0}{2(e^{k_{z,T}t_0} - 1)^2} - 1 \right\}, \quad (\text{B-6}) \end{aligned}$$

fully determine reflection moveout from horizontal interfaces in $v(z)$ VTI media. Hence, for the purpose of migrating horizontal events, the true factorized $v(z)$ medium can be replaced by a homogeneous VTI model with the vertical velocity equal to the average vertical velocity ($\hat{V}_{P0,T}$) above the reflector, the NMO velocity equal to $v_{\text{nmo},T}$, and the parameter η equal to $\hat{\eta}_T$. Note that $\hat{\eta}_T$ depends on the zero-offset time t_0 and, hence, on the depth z_T .

For a migrated image point at half-offset h , the same substitutions can be used to replace the factorized $v(z)$ migration model

above the image point with an equivalent homogeneous model. Therefore, the linearized equation of an image gather for a factorized $v(z)$ medium can be adapted from equation (A-10) for homogeneous media:

$$\begin{aligned} z_M^2(h) &\approx \gamma^2 z_T^2 + h^2 \hat{V}_{P0,M}^2[z_M(h)] \left\{ \frac{1}{v_{\text{nmo},T}^2(z_T)} \right. \\ &\quad \left. - \frac{1}{v_{\text{nmo},M}^2[z_M(h)]} \right\} \\ &\quad + \frac{2h^4}{h^2 + z_T^2} \left\{ \hat{\eta}_M[z_M(h)] \frac{v_{\text{nmo},T}^2(z_T)}{v_{\text{nmo},M}^2[z_M(h)]} \right. \\ &\quad \left. - \hat{\eta}_T[z_T(h)] \frac{v_{\text{nmo},M}^2[z_M(h)]}{v_{\text{nmo},T}^2(z_T)} \right\}, \quad (\text{B-7}) \end{aligned}$$

where $\gamma \equiv \hat{V}_{P0,M}[z_M(h)]/\hat{V}_{P0,T}[z_T(h)]$, \hat{V}_{P0} is the average vertical velocity of the overburden, and the effective NMO velocities and η values are computed from equations (B-5) and (B-6).

When the migration model is close to the true model, the migrated depth is weakly dependent on offset (for a moderate offset range), and the effective quantities for the actual depth $z_M(h)$ can be replaced with those for $z_M(0)$. Then equation (B-7) can be rewritten as

$$\begin{aligned} z_M^2(h) &\approx \gamma^2 z_T^2 + h^2 \hat{V}_{P0,M}^2 \left\{ \frac{1}{v_{\text{nmo},T}^2(z_T)} - \frac{1}{v_{\text{nmo},M}^2[z_M(0)]} \right\} \\ &\quad + \frac{2h^4}{h^2 + z_T^2} \left\{ \hat{\eta}_M[z_M(0)] \frac{v_{\text{nmo},T}^2(z_T)}{v_{\text{nmo},M}^2[z_M(0)]} \right. \\ &\quad \left. - \hat{\eta}_T(z_T) \frac{v_{\text{nmo},M}^2[z_M(0)]}{v_{\text{nmo},T}^2(z_T)} \right\}. \quad (\text{B-8}) \end{aligned}$$

Note, however, that equation (B-8) does not involve the approximation for the effective quantities if the image gather is obtained after migration using a homogeneous VTI medium with the vertical velocity equal to $\hat{V}_{P0}[z(0)]$, NMO velocity equal to $v_{\text{nmo},M}[z(0)]$, and η equal to $\hat{\eta}[z(0)]$.